ChemComm

Accepted Manuscript

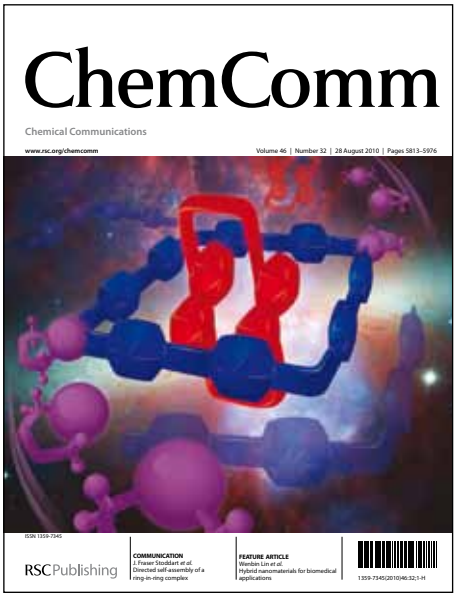

This is an *Accepted Manuscript*, which has been through the RSC Publishing peer review process and has been accepted for publication.

Accepted Manuscripts are published online shortly after acceptance, which is prior to technical editing, formatting and proof reading. This free service from RSC Publishing allows authors to make their results available to the community, in citable form, before publication of the edited article. This *Accepted Manuscript* will be replaced by the edited and formatted *Advance Article* as soon as this is available.

To cite this manuscript please use its permanent Digital Object Identifier (DOI®), which is identical for all formats of publication.

More information about *Accepted Manuscripts* can be found in the **Information for Authors**.

Please note that technical editing may introduce minor changes to the text and/or graphics contained in the manuscript submitted by the author(s) which may alter content, and that the standard **Terms & Conditions** and the **ethical guidelines** that apply to the journal are still applicable. In no event shall the RSC be held responsible for any errors or omissions in these *Accepted Manuscript* manuscripts or any consequences arising from the use of any information contained in them.

Cite this: DOI: 10.1039/c0xx00000x

www.rsc.org/xxxxxx

ARTICLE TYPE

Ultrasensitive Detection of Thrombin Using Surface Plasmon Resonance and Quartz Crystal Microbalance Sensors by Aptamer-Based Rolling Circle Amplification and Nanoparticle Signal Enhancement

Peng He[1], Lijun Liu[1], Wenping Qiao[1], Shusheng Zhang[2]*

Received (in XXX, XXX) Xth XXXXXXXXX 20XX, Accepted Xth XXXXXXXXX 20XX
DOI: 10.1039/b000000x

The surface plasmon resonance (SPR) and quartz crystal microbalance (QCM) aptasensors combined with rolling circle amplification and bio-bar-coded Au NP enhancement have been applied to detect the human α-thrombin for the first time. The assay platform exhibited excellent selectivity and sensitivity with the detection limit as low as 0.78 aM.

Surface plasmon resonance (SPR) represents one of the rapidly advancing technologies for fast, real-time and in situ detection of chemical and biological analytes.[1, 2] The SPR technique is sensitive to the change of refractive index or thickness of the test medium in vicinity of the metal surface, especially for the molecules with larger mass change.[1, 2] However, the inability of conventional SPR to measure extremely small changes in refractive index impedes its further application in ultrasensitive detection. To address this drawback, different amplification strategies were developed. Specifically, Au nanoparticles, as high mass labels, have been extensively used to enhance SPR response. For instance, amplification with secondary antibodies tagged with Au nanoparticles (Au NPs),[3] aggregation of a network of Au NPs,[4] quasi-spherical gold nanoparticles labels,[5] AuNP-polymer growth,[6] and DNA-functionalized Au NPs amplification,[7] all demonstrated the improved detection limits. Nevertheless, the SPR detection can be further improved by combining the novel and powerful signal enhancement methods.

As an advanced molecular amplification technique, rolling circle amplification (RCA), has been attracting much attention due to its unique characteristics such as mild reaction conditions, ease of operation, high efficiency, excellent sensitivity and specificity.[8] Although polymerase chain reaction (PCR) also provides high sensitivity of detection, it requires the highly precise temperature cycling, complex sample preparation and strict laboratory conditions to avoid contamination or false results, which hamper its widespread use for routine analysis.[9] In RCA-based assay, a circular template can be amplified isothermally by certain DNA polymerases such as Phi29 DNA polymerase. The long single-stranded DNA product contains thousands of tandem repeats complementary to the circular template and can serve as the detection sites to enhance signals.[10] Thus, it has been widely employed for the analysis of various target molecules by coupling with electrochemistry,[10, 11] fluorescence,[12] chemiluminiscence,[13] surface-enhanced Raman,[14] and colorimetry.[15] However, to the best of our knowledge, the combination of RCA with SPR for target analytes detection has not been reported.

Quartz crystal microbalance (QCM) is a mass sensing platform based on the piezoelectric properties of quartz crystals. As a different surface-sensitive technology, QCM has also been widely applied in biochemical analysis.[16] Parallel application of SPR and QCM for biochemical analysis is one of the current trends to obtain complementary details and improve the precision with parallel measurements.[3, 17]

Herein, for the first time, the ultrasensitive and versatile SPR and QCM sensing platforms in combination with aptamer-based rolling circle amplification and bio-bar-coded Au NP enhancement were presented for human α-thrombin detection.

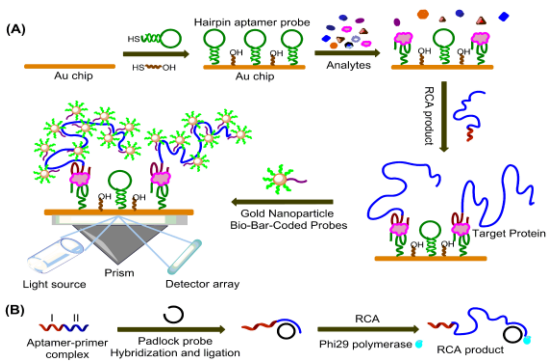

Scheme 1 Schematic representation of the SPR assay for protein detection using sandwiched aptamer recognition mechanism and cascade signal amplification by aptamer-based RCA and bio-bar-coded Au NP enhancement.

As shown in Scheme 1, the hairpin aptamer probe and mercaptohexanol (MCH) are initially immobilized on the chip surface by a Au-S affinity binding (Scheme 1A). As the capture probe, the sequence of the primary aptamer is partially caged in the duplex structure of the stem by hybridization to reduce the

[1]*Key Laboratory of Sensor Analysis of Tumor Marker, Ministry of Education, College of Chemistry and Molecular Engineering, Qingdao University of Science and Technology, Qingdao 266042, P.R.China.*
[2]*College of Chemistry and Chemical Engineering, Linyi University, Linyi 276005, P. R. China. Fax : (+86) 532-84022750; Tel: (+86) 532-84022750; E-mail : shushzhang@126.com*

† Electronic Supplementary Information (ESI) available: Experimental procedures and additional figures. See DOI: 10.1039/b000000x/

nonspecific binding of complex analytes. In the presence of thrombin, the hairpin structure is opened upon interaction of aptamer with the target to form the stable probe-target complex. The aptamer-primer complex (Scheme 1B) contains two domains termed as I, II according to their different functions. The region I is the sequence of the secondary aptamer (colored red) for thrombin. The region II is a primer sequence (colored blue), which could serve as not only the primer of the RCA reaction but also the template for padlock probe ligation. After hybridization and ligation of the padlock probe, a linear RCA reaction could be initiated in the presence of Phi29 DNA polymerase and dNTPs, producing hundreds of tandem-repeat sequences. Then the RCA products are injected into the SPR flow system. The secondary aptamer domain of the products bound to the immobilized protein in a classic sandwich assay format to localize the long single-strand DNA directly to the thrombin. Thus, a large amount of Au NP labeled bio-bar-coded probes are linearly and periodically assembled to the RCA products for amplification of recognition event. The enhancement of the SPR signals is achieved by increasing surface mass and refractive index from clustered AuNP conjugates on the SPR chip. However, for the QCM sensor, signal enhancement is achieved as a result of the mass increase. The multiple signal amplification process are real-timely monitored by SPR and QCM biosensors respectively, which can be used to measure the thrombin concentration in the samples.

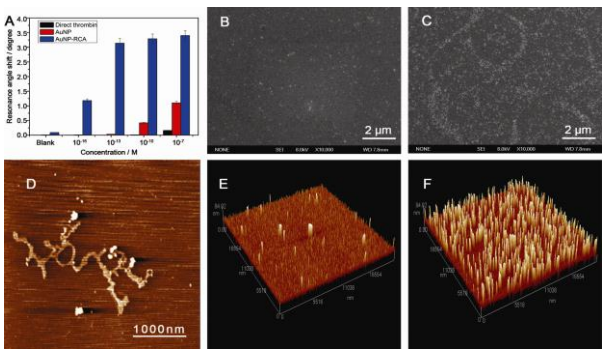

Fig. 1 Signal amplification performance of AuNP-RCA strategy. (A) Comparison of SPR response of direct thrombin binding (black), AuNP amplification (red), and AuNP-RCA amplification (blue) for detection of thrombin. (B, C) SEM images of DNA functionalized AuNPs without RCA and with RCA for detection of thrombin. (D) AFM image of the RCA product. (E, F) AFM images of DNA functionalized AuNPs without RCA and with RCA for detection of thrombin.

To quantify the amplification efficiency, SPR angular shifts for direct target thrombin binding, AuNP amplification, and AuNP-RCA amplification were compared. Fig. 1A compares a series of thrombin solutions measured with SPR angular shifts for each amplification step. In the absence of the amplification, thrombin binding signal was at 1 nM, which is consistent with the literature results by direct SPR analysis.[18] Bio-bar-coded AuNP alone could significantly enhance the responses and reduce the detection limit to about 0.1 pM, showing a 4 orders of magnitude improvement. However, the remarkable amplification performance was obtained with the bio-bar-coded AuNP-RCA method. As shown in Fig. 1C and 1F, a larger scale AuNP could be generated at lower target concentration due to the RCA product (Fig. 1D). The AFM image shows linear long DNA strands (up to a few micrometers). In the presence of 0.1 pM thrombin, a 0.14 degree angular shift was obtained after RCA product binding. The RCA product coverage on the film was about 117 ng cm^{-2}.[6] Upon adding the bio-bar-code AuNPs to the SPR cell, SPR angle rapidly increased with time and the final angle shift resulting from the attachment of AuNP was about 3.03 degree, generating a relatively rigid, and homogeneous surface morphology (Fig. 1F). Moreover, as low as 1 aM target thrombin could be directly detected, which is almost 9 orders of magnitude lower compared with the direct SPR detection. This result stemmed from the bio-bar-code technology that could efficiently avoid cross-reaction (ESI †) and RCA reaction which substantially increased the surface coverage of AuNPs. The SPR angular shifts showed low background response (Fig. 1A, Fig. 2A, and Fig. S5, ESI †), which could be ascribed to the highly specific recognition of the immobilized hairpin-aptamer capture probe to the target, dual-aptamer recognition, and the block of MCH for the nonspecific adsorption.

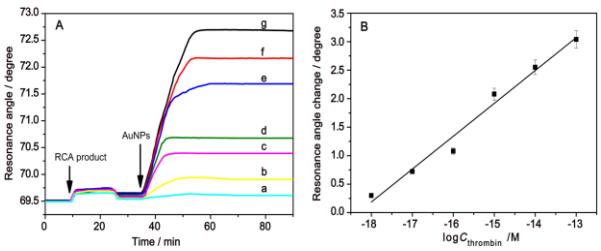

Fig. 2 (A) Real-time resonance angle responses of amplified SPR biosensor for thrombin detection. From a to g: 0, 10^{-18}, 10^{-17}, 10^{-16}, 10^{-15}, 10^{-14}, 10^{-13} M thrombin. (B) Linear relationship between the resonance angle shifts and the target thrombin concentrations. The error bars are standard deviations of three repetitive measurements.

In view of the outstanding ability for signal amplification, the dynamic range of the designed method for detection of thrombin analyte was examined (Fig. 2). The SPR signal was proportional to the logarithm value of thrombin concentration over a 5-decade range from 1 aM to 0.1 pM. The regression equation was $Y = 0.5768 \log_{10} C + 10.5696$ (Y is the SPR angular shifts subtracted the response of the blank solution and C is the concentration of thrombin), with a correlation coefficient of 0.991. The detection limit in this work was calculated to be 0.78 aM based on 3S/N (signal-to-noise), which is lower than those of most reported methods (Table S2, ESI †). The ultrahigh sensitivity could be related to the simultaneous combination of the background response reduction with the signal amplification in the assay. The biosensor surface could be regenerated by injecting 1M HCl into the fluidic channels (Fig. S12, ESI †). After ten regenerations, the aptasensor still retained 92.5% of the original sensor performance, suggesting the reusability of the sensor chip. The decrease in sensor performance might be attributed to the structure degradation of the thrombin binding aptamer during the denaturation and renaturation processes. The relative standard deviation (RSD) for eleven replicate determinations of thrombin with different chips at 100 aM was 8.6%, indicating a good reproducibility of the sensing protocol.

The specificity and the utility for real biological sample analysis were further investigated. As shown in Fig. 3, with the non-target proteins, such as α-fetoprotein (AFP), immunoglobulin

G (IgG), bovine serum albumin (BSA), P53 gene (P53) and lysozyme, no apparent change in the SPR angular shift was observed compared with that of the blank test. However, the presence of target thrombin resulted in the dramatic increase in the SPR signal. Moreover, comparable responses were obtained for human α-thrombin spiked in both buffer and human serum. The background signals gained in human serum slightly increased as compared to those in buffer, which is probably due to the interferences of the complex media. With the standard addition method, the recovery rate was found to vary from 95.6 to 103% (Table S3, ESI †). The high specificity, low matrix effect and acceptable recovery could ensure the practicality of the proposed strategy.

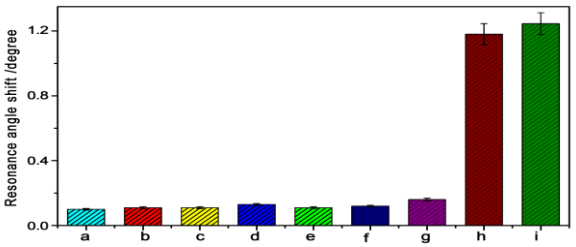

Fig. 3 The resonance angle responses to (a) buffer, (b) AFP, (c) BSA, (d) P53, (e) lysozyme, (f) IgG, (g) human serum samples, (h) thrombin in buffer, (i) thrombin spiked in human serum. The concentration of thrombin: 100 aM, and others: 1 pM. The error bars are standard deviations of three repetitive measurements.

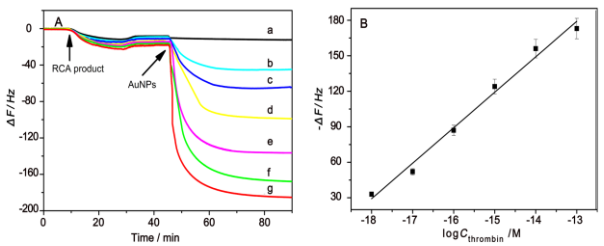

Fig. 4 (A) Real-time frequency responses of amplified QCM biosensor for thrombin detection. From a to g: 0, 10^{-18}, 10^{-17}, 10^{-16}, 10^{-15}, 10^{-14}, 10^{-13} M thrombin. (B) Linear relationship between the frequency shifts and the target thrombin concentrations. The error bars are standard deviations of three repetitive measurements.

The aptamer-based sandwich assay in combination with AuNP-RCA amplification was further implemented for the QCM biosensor. The most common quantification principle for the QCM technique is based on its mass-frequency correlation described by the Sauerbrey equation.[19] The equation can be simply expressed as $\Delta F = -C\Delta m$, where C is a constant dependent on the quartz properties, 56.6 Hz μg^{-1} cm^2 for the 5 MHz AT-cut quartz used here. According to Sauerbrey equation, the resonant frequency shifts (ΔF) on the gold QCM electrode surface is linearly proportional to the change of surface total mass (Δm) on the crystal. In the presence of thrombin, a large amount of AuNP hybridized with the RCA product on the chip surface, leading to a significant ΔF. The QCM biosensor showed different amplified responses to thrombin of various concentrations (Fig. 4A). A linear relationship between the ΔF and the logarithm of thrombin concentrations over a 5-decade range from 1 aM to 0.1 pM was obtained, with a linear correlation coefficient of 0.994 (Fig. 4B). The limit of detection was estimated to be 0.8 aM (S/N = 3). Control experiments were carried out to detect the selectivity of the present aptasensor (Fig. S13, ESI †), the amplified QCM aptasensor exhibited high selectivity. Detection in complex biological media was also performed with the QCM aptasensor by spiking thrombin into 10% human serum. The recoveries varied from 97.6 to 105.2% (Table S4, ESI †). Comparing the results obtained from the SPR and QCM sensor (Fig. S14, ESI †), the linear correlation with R^2 values of 0.993 was achieved. All the results indicated that both biosensors are in line with each other and can be used for the detection of human α-thrombin in the complex biological samples.

In conclusion, the SPR and QCM aptasensor platform which combined the rolling circle amplification technique with the bio-bar-coded Au NPs was developed for the detection of subattomolar human α-thrombin. Both sensor platforms exhibited broad dynamic range, ultrahigh sensitivity, excellent specificity and practical applicability. More importantly, the results implied that the strategy could be applied for the quantitative analysis of DNA, cells and other proteins (e.g. PDGF and avidin) with two or more aptamers, and will be an useful analytical tool in biological research and clinical diagnostics.

This work was supported by the National Natural Science Foundation of China (21227008, 21275086), the National Basic Research Program of China (2010CB732404), and the Program for Changjiang Scholars and Innovative Research Team in University (PCSIRT).

Notes and references

1 (a) W. Knoll, *Annu. Rev. Phys. Chem.*, 1998, **49**, 569; (b) B. A. Snopok, *Theoretical and Experimental Chemistry*, 2012, **48**, 283.
2 (a) J. Homola, *Chem. Rev.*, 2008, **108**, 462; (b) P. M. Boltovets, O. M. Polischuk, O. G. Kovalenko and B. A. Snopok, *Analyst*, 2013, **138**, 480; (c) P. M. Boltovets and B. A. Snopok, *Talanta*, 2009, **80**, 466.
3 (a) L. A. Lyon, M. D. Musick, M. J. Natan, *Anal. Chem.*, 1998, **70**, 5177; (b) Y. Uludag and I. E. Tothill, *Anal. Chem.*, 2012, **84**, 5898.
4 (a) M. Frasconi, R. Tel-Vered, M. Riskin, I. Willner, *Anal. Chem.*, 2010, **82**, 2512; (b) M. Riskin, Y. Ben-Amram, R. Tel-Vered, V. Chegel, J. Almog, I. Willner, *Anal. Chem.*, 2011, **83**, 3082.
5 (a) E. J. Kim, B. H. Chung, H. J. Lee, *Anal. Chem.*, 2012, **84**, 10091; (b) M. J. Kwon, J. Lee, A. W. Wark, H. J. Lee, *Anal. Chem.*, 2012, **84**, 1702.
6 Y. Liu and Q. Cheng, *Anal. Chem.*, 2012, **84**, 3179.
7 (a) E. Golub, G. Pelossof, R. Freeman, H. Zhang, I. Willner, *Anal. Chem.*, 2009, **81**, 9291; (b) L. K. Gifford, I. E. Sendroiu, R. M. Corn, A. Lupták, *J. Am. Chem. Soc.*, 2010, **132**, 9265.
8 D. Y. Liu, S. L. Daubendiek, M. A. Zillman, K. Ryan, E.T. Kool, *J. Am. Chem. Soc.*, 1996, **118**, 1587.
9 (a) D. A. Giljohann, C. A. Mirkin, *Nature*, 2009, **462**, 461; (b) C. A. Heid, J. Stevens, K. J. Livak, P. M. Williams, *Genome Res.*, 1996, **6**, 986.
10 (a) H. Ji, F. Yan, J. Lei, H. Ju, *Anal. Chem.*, 2012, **84**, 7166 (b) L. Zhou, L. Ou, X. Chu, G. Shen, R. Yu, *Anal. Chem.*, 2007, **79**, 7492.
11 W. Cheng, F. Yan, L. Ding, H. Ju, Y. Yin, *Anal. Chem.*, 2010, **82**, 3337.
12 (a) S. A. McManus, Y. Li, *J. Am. Chem. Soc.*, 2013, **135**, 7181; (b) Q. Xue, L. Wang W. Jiang, *Chem. Commun.*, 2012, **48**, 3897.
13 S. Bi, T. Zhao, B. Luo, J. Zhu, *Chem. Commun.*, 2013, **49**, 6906.
14 (a) J. Hu, C. Zhang, *Anal. Chem.*, 2010, **82**, 8991; (b) S. Ye, Y.Yang, J. Xiao, S. Zhang, *Chem. Commun.*, 2012, **48**, 8535.
15 (a) L. Tang, Y. Liu, M. M. Ali, D. K. Kang, W. Zhao, J. Li, *Anal. Chem.*, 2012, **84**, 4711; (b) M. M. Ali, Y. F. Li, *Angew. Chem., Int. Ed.*, 2009, **48**, 3512.
16 (a) G. Papadakis, A. Tsortos, E. Gizeli, *Nano Lett.*, 2010, **10**, 5093. (b) W. Tang, D. Wang, Y. Xu, N. Li, F. Liu, *Chem. Commun.*, 2012, **48**, 6678.
17 X. Su, C. Lin, S. J. O'Shea, H. F. Teh, W. Y. X. Peh, J. S. Thomsen, *Anal. Chem.*, 2006, **78**, 5552.
18 Y. Bai, F. Feng, L. Zhao, C. Wang, H. Wang, M. Tian, J. Qin, Y. Duan, X. He, *Biosens. Bioelectron.*, 2013, **47**, 265.
19 G. Z. Sauerbrey, *Z. Phys. A: Hadrons Nuclei*, 1959, **155**, 206.